Leikina et al., http://www.jcb.org/cgi/content/full/jcb.201207012/DC1

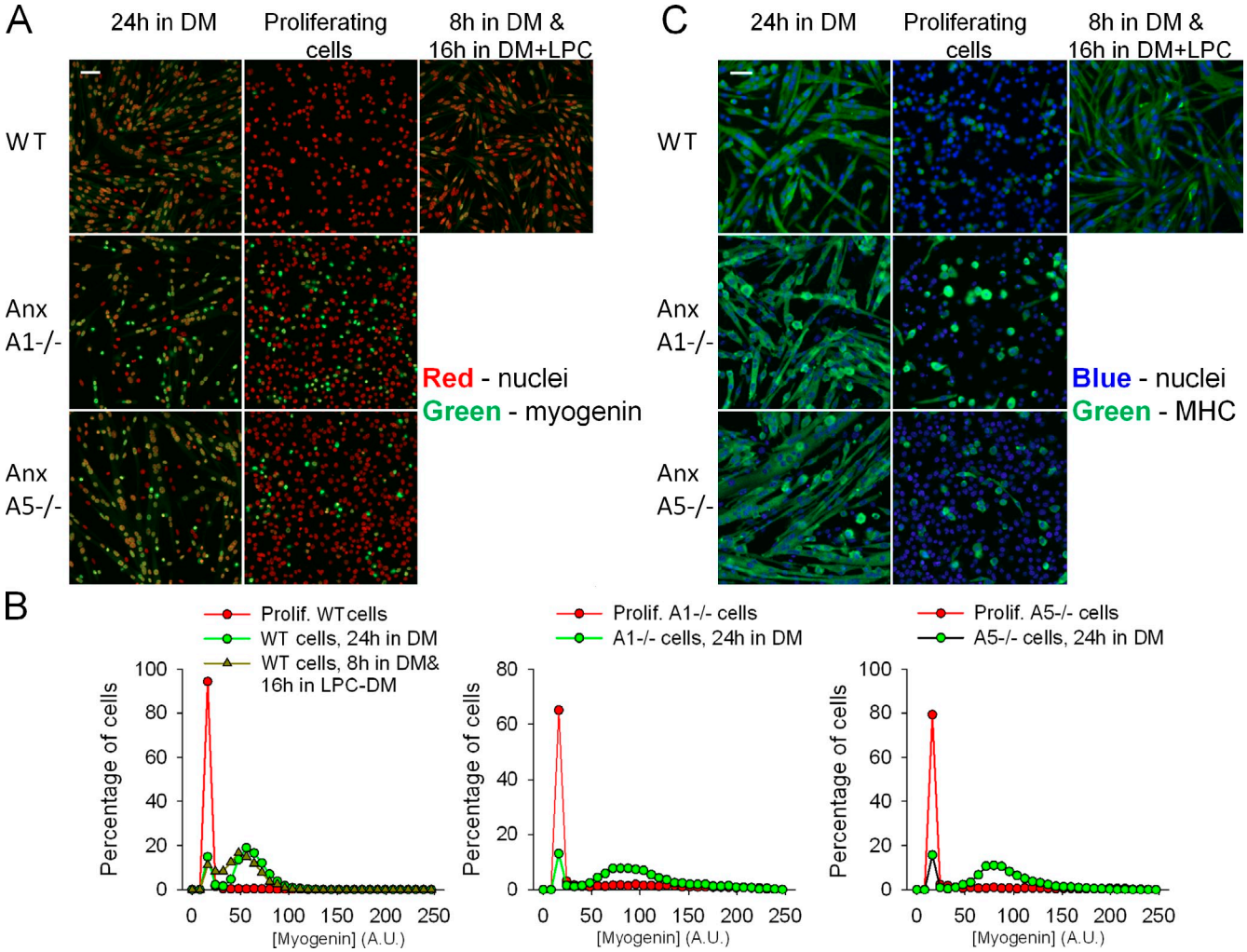

Figure S1. **Neither the lack of Anx A1 or A5 nor 16 h incubation with LPC blocks expression of myogenic markers myogenin and MHC in primary myoblasts.** (A and C) We compared expression of myogenin (A) and MHC (C) in $A1^{-/-}$ cells, in $A5^{-/-}$ myoblasts, and in WT myoblasts incubated or not with LPC by immunofluorescence microscopy (see Materials and methods). The cells were analyzed after 24 h in DM. Bars, 50 µm. (B) We used Hoechst staining to automatically create a region of interest for each cell nucleus and measured mean pixel intensity for anti-myogenin staining within these regions. This experiment has been completed once with numbers of analyzed cell nuclei between 2,353 and 5,739 for different experimental conditions. We did not quantify MCH expression in the images because cytosolic distribution of MHC complicates their automated analysis. However, qualitatively MCH labeling in Anx-deficient cells appears to be similar to that in WT cells.

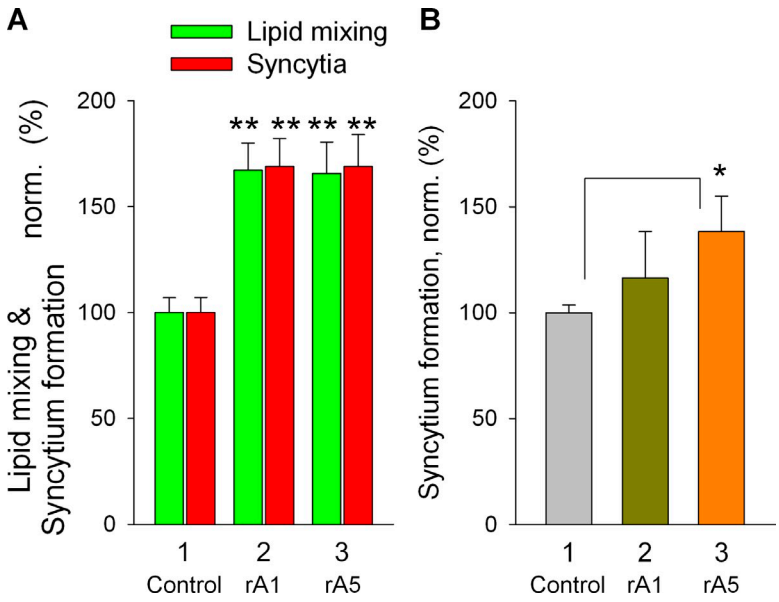

Figure S2. **rA1 and rA5 promote myotube formation by C2C12 cells and primary myoblasts.** (A) rA1 and rA5 (2 and 3, respectively) promote myotube formation by C2C12 cells assayed as lipid mixing (green) and syncytium formation (red). (B) rA1 and rA5 promote syncytium formation by primary myoblasts. (A and B) Fusion extents are normalized to those observed in the control experiments (1). (2 and 3) rA1 and rA5 applied for the last 3 h. Means ± SEM. Levels of significance relative to 1 are shown: **, P < 0.01; *, P < 0.05.

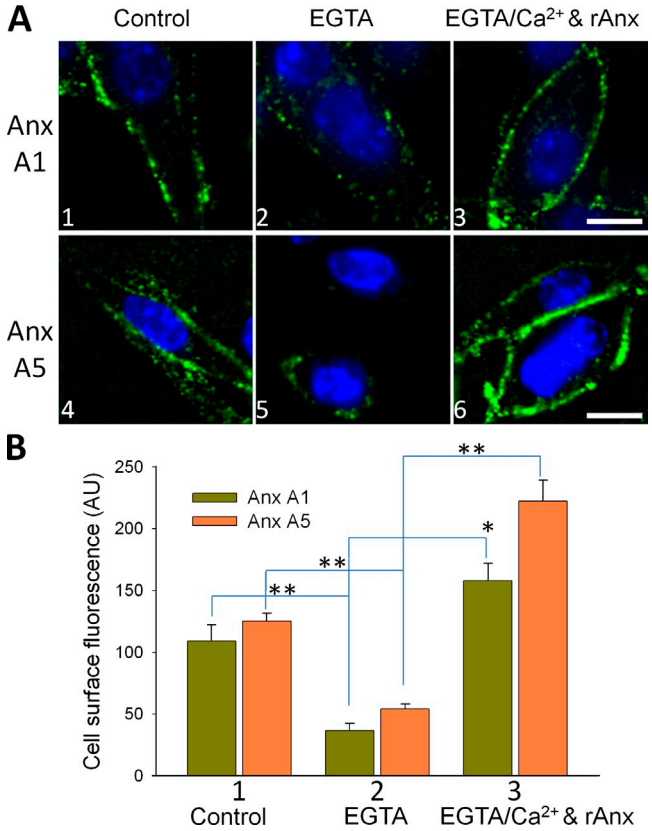

Figure S3. **Loss of Anx A1 and A5 at the surface of primary myoblasts after EGTA application and their recovery after the application of Ca^{2+} and recombinant Anxs.** (A) Anx A1 (1 and 2) and A5 (3 and 4) were detected by immunofluorescence microscopy with corresponding antibodies for nonpermeabilized primary myoblasts 24 h after placing the cells in DM (2 and 4). Bars, 10 µm. (B) Cell surface fluorescence was quantified for 16 cells for each condition. Means ± SEM. Levels of significance relative to 1 are shown: **, P < 0.01; *, P < 0.05.

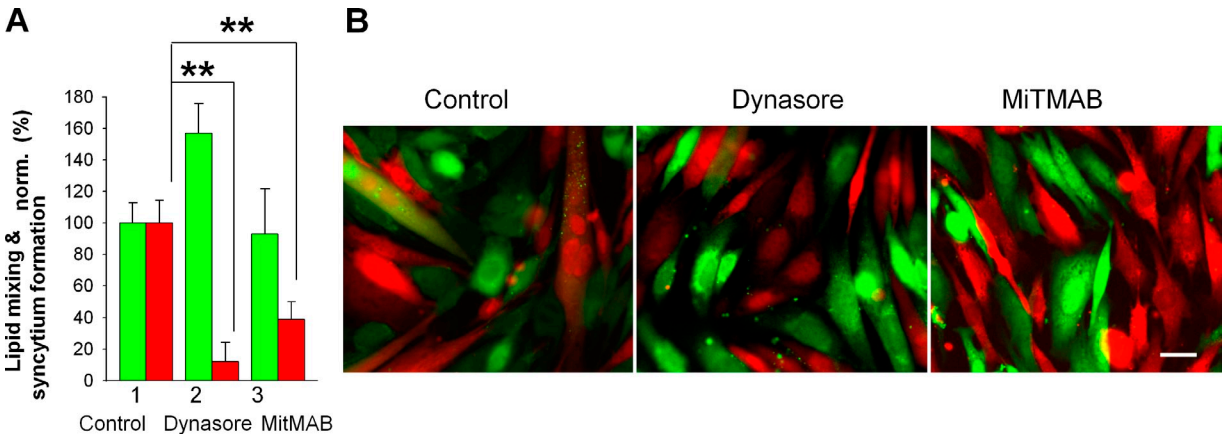

Figure S4. **DNM inhibitors block myotube formation by C2C12 cells downstream of lipid mixing but before fusion pore opening.** (A) Blocking DNM GTPase activity with 80 µM dynasore (2) and 25 µM MitMAB (3) applied at the time of LPC removal inhibits myotube formation but not lipid mixing. Fusion extents quantified 30 min after LPC removal as lipid mixing (green) and syncytium formation (red) were normalized by those for the untreated cells released from LPC block (1). Means ± SEM ($n \geq 3$). Levels of significance relative to 1 are shown: **, $P < 0.01$. (B) Images showing fluorescence of the coplated cells prelabeled with either green or orange cell trackers. At the time of LPC removal the cells were treated with 80 µM dynasore (middle) and 25 µM MitMAB (right). Images were taken 30 min later. We observed no redistribution of the cell tracker–labeled cytosolic proteins between the cells treated with DNM inhibitors, suggesting that these inhibitors block fusion at a stage that precedes formation of fusion pores large enough to pass our cytosolic probes. Bar, 50 µm.

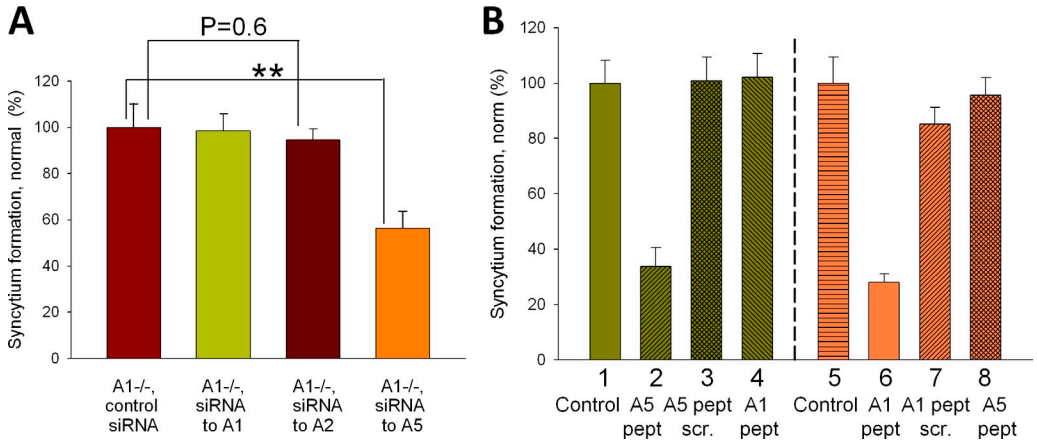

Figure S5. **Myotube formation by the primary myoblasts lacking either Anx A1 or A5 is not affected by siRNA and N-terminal peptides targeting the missing Anx.** (A) Syncytium formation by Anx $A1^{-/-}$ myoblasts was inhibited by siRNA targeting Anx A5 but not affected by siRNAs targeting either Anx A1 or Anx A2. 100 pM of siRNA. Syncytium formation was scored 24 h after placing the cells into DM and normalized to that for Anx $A1^{-/-}$ myoblasts transfected with negative control siRNA. All results are means ± SEM ($n \geq 3$). Only transfection with siRNA to Anx A5 resulted in a statistically significant fusion inhibition (**, $P < 0.01$). Finding that siRNA targeting Anx A2 does not affect syncytium formation by Anx $A1^{-/-}$ myoblasts ($P = 0.6$) argues against involvement of this Anx in murine myoblast fusion. (B) The peptides (final concentration of 100 µg/ml) were applied 20 h after the cells were committed to myogenesis by placement into DM, and fusion was assayed 4 h later as the percentage of cell nuclei present in myotubes compared with the total number of cell nuclei. 1–4, myoblasts from Anx A1–deficient mouse. 1, no peptides added; 2–4, fusion was inhibited by N-peptide to Anx A5 (2) but not by its scrambled version (3) nor by Anx A1 N-peptide (4); 5–8, myoblasts from Anx A5–deficient mouse; 5, no peptides added; 6–8, fusion was inhibited by N-peptide to Anx A1 (6) but not by its scrambled version (7) nor by Anx A5 N-peptide (8). Means ± SEM ($n \geq 3$).

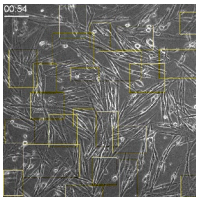

Video 1. **Largely synchronized fusion of primary myoblasts from WT mice.** Primary myoblasts from WT mice were incubated for 8 h in DM and then for 16 h in DM supplemented with LPC. At *t* = 0 the cells were washed to remove LPC and lift the block to cell fusion and transferred into a microscope stage culture dish incubator for imaging. Images were analyzed by time-lapse phase-contrast microscopy using a custom setup as described in Materials and methods. Frames were taken every 2 min for 70 min. Time since removal of LPC is indicated as hours:minutes. Regions where myoblast fusion occurs are marked by yellow rectangles. Bar, 100 µm.

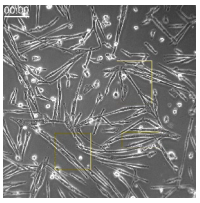

Video 2. **Control experiment that shows a few fusion events between WT primary myoblasts observed within the same time interval from 24 to 25 h in DM as in Video 1 for the cells that were not treated with LPC.** Primary myoblasts from WT mice were incubated for 24 h in DM and then transferred into a microscope stage culture dish incubator for imaging. Images were analyzed by time-lapse phase-contrast microscopy using a custom setup described in Materials and methods. Frames were taken every 2 min for 66 min. Time since transfer onto microscope stage is indicated as hours:minutes. Regions where myoblast fusion occurs are marked by yellow rectangles. Bar, 100 µm.